Journal of Genetic Engineering and Biotechnology 23 (2025) 100496

Contents lists available at ScienceDirect

Journal of Genetic Engineering and Biotechnology

journal homepage: www.elsevier.com/locate/jgeb

Co-expression of HIF1A with multi-drug transporters (P-GP, MRP1, and BCRP) in chemoresistant breast, colorectal, and ovarian cancer cells

Sudipta Deb Nath [a], Md Tamzid Hossain Tanim [a], Md. Mahmudul Hasan Akash [a], Mohammad Golam Mostafa [b,*], Abu Ashfaqur Sajib [a,**]

[a] Department of Genetic Engineering & Biotechnology, University of Dhaka, Dhaka 1000, Bangladesh
[b] Anowara Medical Services, Dhaka 1205, Bangladesh

ARTICLE INFO

Keywords:
HIF1A
ABC transporters
Cancer chemoresistance
Co-expression
BCRP, P-GP, MRP1

ABSTRACT

Therapeutic resistance poses a significant challenge in treating most cancers and often leads to poor clinical outcomes and even treatment failure. One of the primary mechanisms that confer multidrug resistance phenotype to cancer cells is the hyperactivity of certain drug efflux transporters. P-GP, MRP1, and BCRP are the key ABC efflux pumps that collectively extrude a broad spectrum of chemotherapeutic drugs. Besides, HIF1A, a master transcription regulatory protein, is also associated with cancer development and therapeutic resistance. Thereby, this study aimed to delve into the mechanisms of drug resistance, specifically focusing on HIF1A-driven overexpression of ABC transporters. A total of 57 chemoresistant and 57 paired control tissue samples (breast, colorectal, and ovarian) from Bangladeshi cancer patients were analyzed to determine the co-expression level of ABC transporters and HIF1A. Molecular docking was also conducted to evaluate the interactions of HIF1A protein and hypoxia response element (HRE) sequences in the promoter regions transporter genes. This study revealed that HIF1A is significantly overexpressed in chemoresistant tissues, suggesting its pivotal role in chemoresistance mechanisms across malignancies and its potential as a target to overcome therapeutic resistance. The findings from this study also suggest a direct upregulation of *ABCB1*, *ABCC1*, and *ABCG2* transcription by HIF1A in chemoresistant cancer cells by binding to the HRE sequence in the promoter regions. Thus, inhibition of these interactions of HIF1A appears to be a promising approach to reverse chemoresistance. The findings of this study can serve as a foundation for future research, resolving molecular intricacies to improve treatment outcomes in chemoresistant patients.

1. Introduction

Among the current cancer treatment techniques, chemotherapy stands out as the most potent and efficient approach for those with limited or unsatisfactory responses to surgery or radiation therapy.[1–2] Anthracyclines, taxanes, antimetabolites like antifolates and nucleoside analogs, cyclin-dependent kinase inhibitors (CDKIs), tyrosine kinase inhibitors (TKIs), platinum-derived compounds, and vinca alkaloids are some of the most extensively used chemotherapeutic agents across various cancer types.[3] Though the development of novel antineoplastic drugs has enhanced the overall efficacy of cancer treatment, multidrug resistance remains a particularly formidable issue, especially in addressing metastatic cancers.[4–5] Drug resistance mechanisms contribute to over 90 % of treatment failures in metastatic malignancies.[6–7] Approximately 30 % of women diagnosed with early-stage breast cancer encounter relapse, along with therapeutic resistance in at least 25 % of cases, and this is attributed to the elevated mortality rate associated with breast cancer.[8] Nearly half of the patients experiencing recurrent disease indicate that multidrug resistance is a predominant trait for colorectal cancer.[9] A study also revealed that 20 % to 30 % of individuals diagnosed with ovarian cancer exhibit chemoresistance, and a notable portion of primary responders to chemotherapy eventually experience the reversion of the disease.[10]

When subjected to chemotherapy, cancer cells can exhibit multiple mechanisms of multidrug resistance.[4] Among these mechanisms, chemoresistance mediated by ATP-binding Cassette (ABC) transporters is one of the crucial processes. Among all the 49 ABC transporters, P-GP (*ABCB1*), MRP1 (*ABCC1*), and BCRP (*ABCG2*) play a collective role in

* Corresponding author at: Anowara Medical Services, Dhaka 1205, Bangladesh.
** Corresponding author at: Department of Genetic Engineering & Biotechnology, University of Dhaka, Dhaka 1000, Bangladesh.
E-mail addresses: dmgm.path@gmail.com (Md.M.H. Akash), dmgm.path@gmail.com (M. Golam Mostafa), abu.sajib@du.ac.bd (A.A. Sajib).

https://doi.org/10.1016/j.jgeb.2025.100496
Received 10 January 2025; Received in revised form 9 April 2025; Accepted 10 April 2025

exporting 80 % of all drugs out of cells.[11–13] P-GP, MRP1, and ABCG2 can mediate the transport of a broad spectrum of agents, including topoisomerase inhibitors, anthracyclines, antimetabolites, vinca alkaloids, TKI, CDKI, mitoxantrone,etc.[14–22] Overexpression of these proteins and their contribution to therapeutic non-responsiveness have been documented across various hematological and solid tumors, including non-small cell lung cancer (NSCLC), leukemia, neuroblastomas, ovarian, prostate, colorectal, pancreatic, and breast cancers.[23–36]

However, overexpression of ABC transporters in cancer cells, regulated by hypoxia-inducible factor 1 alpha (HIF1A), has been a prominent topic for years. HIF1 functions as a master regulator of gene expression which helps cells to adapt to conditions like hypoxia and to govern cellular responses to oxygen levels within mammals.[37–40] The alpha subunit of HIF1 is capable of triggering the transcription of more than 40 genes by binding to the hypoxia response elements (HREs) (5′ −RCGTG-3′ (where R = A or G)).[41–42] Dysregulated expression of HIF1A has a noteworthy role in cancer biology.[43] This involves biological processes like tumor angiogenesis and invasion, energy metabolism, and cell survival.[43–44] Moreover, decreased oxygen in cells radically influences the activation of signaling pathways related to chemoresistance mechanisms.[45] This results in enhanced expression of HIF1A in drug-resistant tumors.[46] Numerous studies found elevated HIF1A levels in various types of malignant tumors, including breast cancer, colorectal cancer, hepatocellular carcinoma, glioblastoma, NSCLC, cervical cancer, and ovarian cancer.[47–48]

Some studies previously investigated the association of HIF1A and P-GP in the progression of drug resistance.[49–51] Moreover, another study has shown that hypoxia-induced activation of HIF1A leads to the acquisition of chemoresistant properties in pancreatic cancer cells through the elevation in BCRP expression.[52] Besides, HIF1A has been predicted to be a regulator of MRP1 expression as well.[53] However, the intricate relationship and dynamics between these ABC transporters and HIF1A as well as how they can function synergistically to aid in the development of therapeutic resistance still remains enigmatic. Therefore, this study aims to shed light on the expression patterns of HIF1A in chemoresistant breast, colorectal, and ovarian cancer cells obtained from Bangladeshi cancer patients and to investigate the co-expression profiles of ABC transporter proteins (P-GP, MRP1, and BCRP) with HIF1A by employing both experimental and bioinformatic methods. The findings from this study will contribute to unraveling the underlying mechanisms behind ABC drug transporter-mediated therapeutic resistance and identify potential therapeutic targets for overcoming chemoresistance.

2. Materials and methods

2.1. Inclusion criteria for experimental samples and development of the questionnaire

For inclusion, the breast, colorectal, and ovarian cancer patients had to meet the criteria of having a previous history of non-responsiveness to chemotherapeutic drugs. Besides, a questionnaire was developed to collect sociodemographic and clinical information from the participants. The questionnaire had seven variables: address, age, gender, diagnosis, differentiation, grade, and stage.

2.2. Immunofluorescence imaging

2.2.1. Sample collection

A total of 57 paired tissue samples (chemoresistant tumor and control) were collected from 28 individuals with breast cancer, 21 individuals with colorectal cancer, and 8 individuals with ovarian cancer. We have selected these cancers because their occurrence contributes to the development of another one. These malignancies share family histories.[54,55] Cancerous and corresponding control tissue morphology were determined by an experienced histopathologist using hematoxylin and eosin (H&E) staining. During data collection, the participants were provided with a clear insight into the aims and objectives of this study. Additionally, strict measures such as private interviews were implemented to maintain the anonymity of the patients. The cancer tissues and corresponding controls were immediately immersed in a 10 % formalin solution following excision from the patients.

2.2.2. Preparation of formalin-fixed, paraffin-embedded (FFPE) tissue

Tissues were processed using an automated vacuum tissue processor (ASP6025, Leica Biosystems), following a 12-hour protocol outlined below: the tissues were incubated in 10 % formalin for 1.5 h, followed by sequential rinsing in 70 % isopropanol (for 30 min), 90 % isopropanol (for 30 min), 100 % isopropanol (for 1 h), 100 % isopropanol (for 30 min), 100 % isopropanol (for 1.5 h), 100 % isopropanol (for 30 min), and xylene (twice for 45 min each, and once for 1.5 h). All these steps were conducted at 37 °C. The tissues then underwent paraffin baths three times for 1 h each at 65 °C.

2.2.3. Deparaffinization and rehydration of the FFPE tissues

The FFPE tissue blocks were sectioned into slices of 3 μm thickness using a rotary microtome (RM2235, Leica Biosystems) and sections were delicately positioned onto positively charged (electrostatic) glass slides (10010–882; VWR). The slides with tissue sections were then submerged thrice in xylene for 5 min duration each andtwice in 100 % ethanol (100983; Merck) for 3 min each. Afterwards, the tissue sections were sequentially submerged into 95 %, 70 %, and 50 % ethanol for 3 min each.

2.2.4. Antigen retrieval, permeabilization, and blockage of nonspecific binding

Following rehydration, the tissue sections were transferred in an incubation chamber containing a tri-sodium citrate buffer (10 mM Sodium Citrate, pH 6.0), with 0.05 % (w/v) Tween® 20). To reactivate the antigens, the slides were heated at 100 °C for 3.5 min, followed by 80 °C for an additional 20 min. After the samples reached room temperature, the slides were briefly rinsed with flowing distilled water for 5 min. The boundaries around the tissue sections were then marked by a hydrophobic-liquid blocker super PAP pen (008899; Thermo Fisher Scientific).

Then the tissue sections on the slides were immersed in phosphate buffer saline (PBS) (137 mM NaCl, 2.7 mM KCl, 10 mM Na_2HPO_4, 1.8 mM KH_2PO_4, and distilled water with the pH level adjusted to 7.4) with 0.1 % (w/v) Triton X-100 for 20 min. Following the immersion step, the tissue sections underwent three sequential washes with PBS, each taking 10 min.

The tissue sections on slides were incubated with 40 μl of PBS containing 0.3 M glycine (194825; MP Biomedicals) for 20 min followed by three times wash with PBS for 10 min each. Then these were incubated for another 30 min with 5 % normal goat serum (NGS) (ab7481; Abcam) in PBS.

2.2.5. Incubation with primary Abs (1° Abs)

Subsequently, the tissue sections were treated with 1° Abs in a solution of 3 % NGS in PBS. The following 1° Abs were used: rabbit Anti-P-GP polyclonal Ab (ab235954; Abcam; diluted 1:1000), rabbit Anti-MRP1 recombinant monoclonal Ab (ab233383; Abcam; diluted 1:200), rabbit Anti-BCRP recombinant monoclonal Ab (ab229193; Abcam; diluted 1:200), and mouse Anti-HIF1A monoclonal Ab (ab8366; Abcam; diluted 1:200). Moreover, tissue quality assessment involved incubation of one section for each sample with rabbit Anti-Pan-Cadherin polyclonal Ab (4068; Cell Signaling Technology®; diluted 1:200) (Supplementary Fig. 1). To ascertain high cell proliferation across the cancerous tissues, mouse Anti-Ki-67 monoclonal Ab (ab238020; Abcam; diluted 1:500) was used (Supplementary Fig. 2). To ensure the specific binding ability of 1° Abs for ABC transporters, non-specific rabbit (DA1E) monoclonal Ab IgG XP® isotype control (3900; Cell Signaling

Technology®; diluted 1:1500) was applied on an individual section (Data not shown).This incubation lasted overnight at 4 °C. After incubation, the slides containing tissue sections underwent four eight-minute washes with PBS containing 0.1 % Tween-20 (PBS-T).

2.2.6. Incubation with labeled secondary Abs (2º Abs)

Following incubation with 1º Abs, all the succeeding procedures were conducted in dark. The tissue sections were treated with appropriate 2ºAbs diluted in PBS containing 3 % NGS at room temperature for 1 h. The 2º Abs used were Alexa Fluor® 488-labeled Goat Anti-Rabbit IgG H&L polyclonal Ab (ab150077; Abcam) and Alexa Fluor® 555-labeled Goat Anti-Mouse IgG H&L polyclonal Ab (ab150114; Abcam). For the anti-ABC transporters, anti-HIF1A and the IgG 1º Abs, the 2º Abs were diluted at a ratio of 1:2000, whereas in the case of anti-pan-cadherin and anti-Ki67 Abs, the dilution was 1:1000. Moreover, to assess the of fluorescence of Alexa Fluor® 555, separate sections from all samples were treated with Anti-HIF1A along with goat Anti-Mouse IgG, (H + L) horseradish peroxidase (HRP) conjugated polyclonal Ab (another 2º Ab without fluorophore) (31430; Invitrogen; ThermoFisher Scientific; diluted 1:1500) (Data not shown). As a control, one tissue section from all samples was treated only with NGS in PBS (without 1º Abs) and then the 2º Ab (Data not shown). The tissue sections then underwent four eight-minute washes with PBS-T in a dark box. A mounting medium with 4′,6-diamidino-2-phenylindole (DAPI) (ab104139, Abcam) was used and the labeled tissue sections were stored in non-transparent sealed boxes at 4 °C.

2.2.7. Fluorescence microscopy and imaging

The stained tissue specimens were examined using a widefield fluorescence microscope (EVOS FL, Thermo Fisher Scientific) utilizing objective lenses with various magnifications (10×, 20×, and 40 ×), combined with a 10 × eyepiece lens. To facilitate the visualization of different protein expressions, specific band pass filter sets (RFP and GFP) were used, while the DAPI filter was used for the visualization of nuclear staining. Three randomly captured images were selected from each tissue section in the imaging process.

2.2.8. Cell and protein expression counting

Cell quantification was manually conducted using ImageJ software.[56] The initial step involved the enumeration of nuclei, individual red, and individual green expressions within the captured images. Afterwards, to quantify the co-expression among the cell population, a comprehensive cell count was carried out with the colors merged in the ImageJ software. In order to minimize potential biasness during the counting process, two independent individuals counted the cells and protein expressions separately.

2.3. Statistical analysis

Data analysis was conducted using GraphPad Prism 9.5.0 and IBM SPSS Statistics v25. Sociodemographic and clinical data of the patients were presented with frequencies, percentages, mean and standard deviation (sd) (Table 1). To standardize the evaluation of protein expressions, relative expression in percentage (%) was calculated. Relative expression in cells (%) = Relative ratio of expression in cells * 100. Relative ratio of expression in cells = Protein expression count / Total cell count. For HIF1A expression, three technical replicates were considered. The ratios from technical replicates were averaged for accuracy. Co-expression counts, such as ABC transporter-HIF1A in the same cells, were similarly transformed into relative co-expression in percentage (%) {Relative co-expression in cells (%) = (Cell number of co-expression / Cell number of specific ABC transporter expression) * 100}. To examine the Gaussian distribution of the ratios, normality tests were performed using D'Agostino & Pearson, Anderson-Darling, Shapiro-Wilk, and Kolmogorov-Smirnov tests (Supplementary table 1, 2, 3, 7, 8, 9). A P value of > 0.05 indicated normal distribution. If any of these tests failed to demonstrate normal distribution, the data was considered as non-normal data. For the non-normally distributed data, the Wilcoxon signed-rank test for paired samples was applied, while the paired samples *T*-test was performed for the normally distributed data. In these cases, P values < 0.05 were considered statistically significant. Moreover, the link between independent expression of ABC transporters and HIF1A was evaluated through simple linear regression analysis. Regarding the relationship between patient data and expression of proteins in chemoresistant tissues, Pearson's correlation coefficient (for normally distributed numerical data), Spearman correlation (for non-normally distributed numerical data), independent samples *T*-test (for variables with two categories and normally distributed numerical data), Mann–Whitney *U* test (for variables with two categories and non-normally distributed numerical data), ANOVA (for variables with more than two categories and normally distributed numerical data), and Kruskal–Wallis test (for variables with more than two categories and non-normally distributed numerical data) were used.

Table 1
Clinical information on chemoresistant breast, colorectal, and ovarian cancer patients.

Cancer type	Breast Cancer	Colorectal Cancer	Ovarian Cancer
Sample number	28	21	8
Age (mean ± sd)	50.29 ± 13.35	35.24 ± 11.56	53.13 ± 11.52
Diagnosis			
Infiltrating ductal carcinoma	26 (92.86 %)	–-	–-
Ductal carcinoma in situ	1 (3.57 %)	–-	–-
Infiltrating ductal and lobular carcinoma	1 (3.57 %)	–-	–-
Adenocarcinoma	–-	21 (100.00 %)	–-
Papillary serous carcinoma	–-	–-	7 (87.50 %)
Squamous cell carcinoma	–-	–-	1 (12.50 %)
Differentiation			
Well	–-	10 (50.00 %)	–-
Moderate	24 (88.89 %)	8 (40.00 %)	1 (12.50 %)
Poor	3 (11.11 %)	2 (10.00 %)	7 (87.50 %)
Grade			
I	–-	10 (50.00 %)	–-
II	24 (88.89 %)	8 (40.00 %)	1 (12.50 %)
III	3 (11.11 %)	2 (10.00 %)	7 (87.50 %)
T staging			
1	11 (39.29 %)	1 (5.00 %)	1 (16.67 %)
2	11 (39.29 %)	7 (35.00 %)	–-
3	2 (7.14 %)	11 (55.00 %)	5 (83.33 %)
4	3 (10.71 %)	1 (5.00 %)	–-
Tis	1 (3.57 %)	–-	–-
N staging			
0	15 (57.69 %)	10 (52.63 %)	1 (33.33 %)
1	2 (7.69 %)	4 (21.05 %)	2 (66.67 %)
2	5 (19.23 %)	5 (26.32 %)	–-
3	4 (15.38 %)	–-	–-

2.4. Bioinformatic analyses to identify the interplay between HIF1A and ABC transporters

2.4.1. HIF1A structure prediction

The amino acid (AA) sequence of HIF1A was retrieved from UniProt, and the 3D structure was modeled using GalaxyTBM option within the GalaxyWEB online platform.[41,57] The protein model validation involved the generation of a Ramachandran plot utilizing the PROCHECK function within the SAVES v6.0 web-platform.[58]The qualitative Model Energy ANalysis (QMEAN) tool in SWISS-MODEL was also used to assess the Q-mean score for the predicted protein model.[59] Lastly, the

structural integrity was further inspected by determining the Z-score with ProSA-web.[60]

2.4.2. Identification of HRE sequence within the promoter regions of respective transporter genes and 3D modeling of DNA

Directional orientation of the transporter genes within the genome directed our search for their promoters in NCBI Gene.[61] The HRE sequence, 5′-RCGTG- 3′ (where R = A or G) was identified upstream of the 5′ end (promoter area) of the genes. The 3D modeling of DNA involved 50 nucleotide bases preceding and following the HRE region, and the modeling was accomplished using the 'DNA Sequence to Structure' tool in the Supercomputing Facility for Bioinformatics & Computational Biology, IIT Delhi web-based platform.[62]

2.4.3. Molecular docking of selected region inside HIF1A and HRE sequences in the promoters of ABC transporter genes

To evaluate the binding ability, the 3D structures of HIF1A from 2.4.1 and DNAs from 2.4.2 were subjected to molecular docking analyses by HADDOCK 2.4.[63] In total, 3 docking simulations were performed, comprising each transporter gene (*ABCB1*, *ABCC1*, and *ABCG2*) with the AA sequence of 21–30, binding site ofHIF1A. All the docking parameters were set as default, and the scores provided by HADDOCK

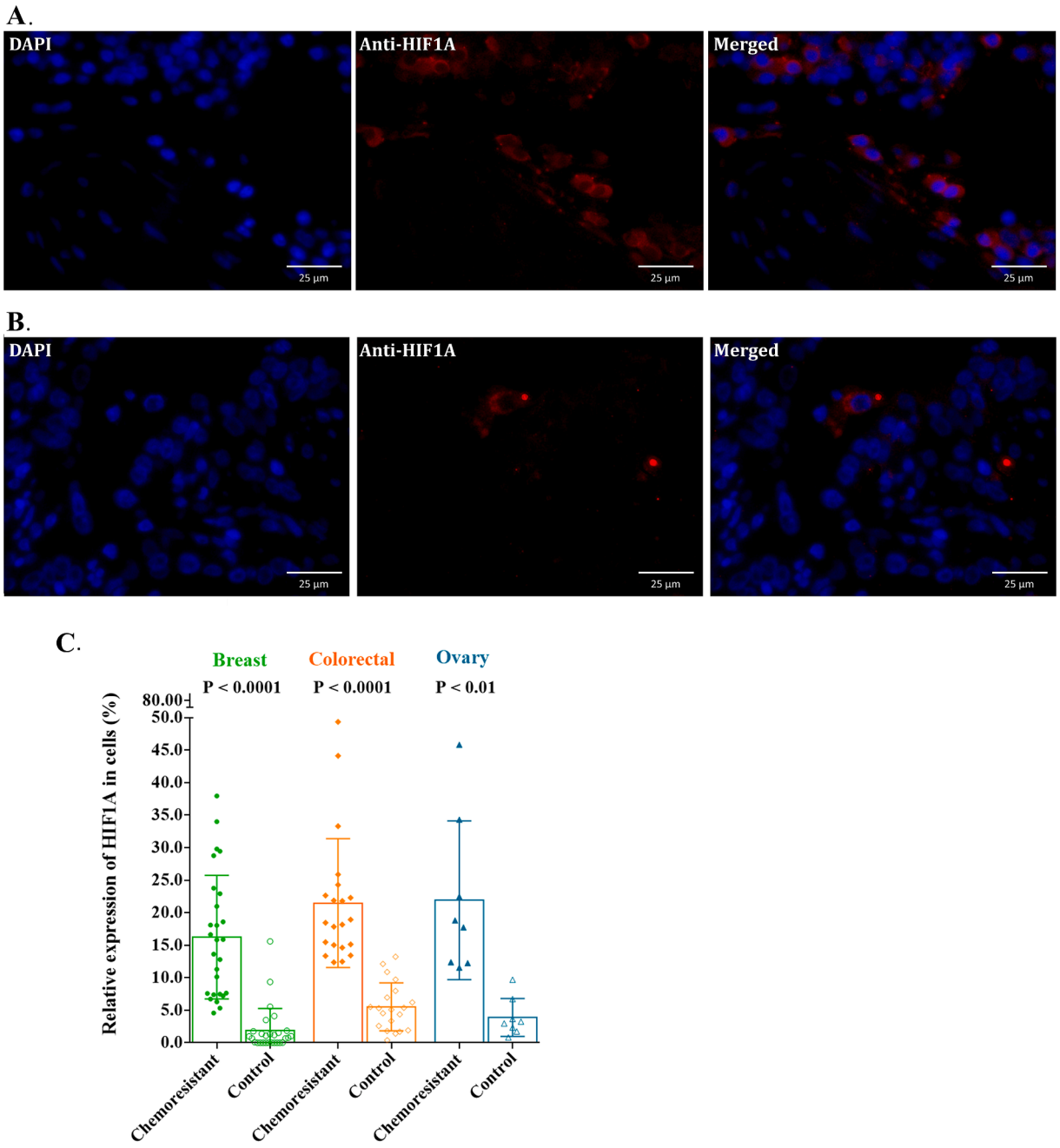

Fig. 1. Expression profiles of HIF1A in chemoresistant breast, colorectal and ovarian cancer tissues. Fig. 1A shows the expression of HIF1A (red) in chemoresistant cancer tissue. Fig. 1B shows the expression of HIF1A (red) in paired control tissue. Fig. 1C shows the comparison of HIF1A expression between chemoresistant and adjacent control tissues. The X-axis represents breast (pink), colorectal (blue), and ovarian (green) cancers. The Y-axis denotes the relative expression of HIF1A in cells in percentage. Wilcoxon signed-rank test for paired samples was conducted to validate the significance of differences for breast, colorectal, and ovarian cancers. Nuclear DNA were stained with DAPI (blue). The scale bar is 25 µm. (For interpretation of the references to colour in this figure legend, the reader is referred to the web version of this article.)

2.4 were collected for further assessment. Docking outcomes with negative Z-scores were considered indicative of effective binding. Docking results were visualized by ChimeraX.[64]

3. Results

3.1. Information on chemoresistant breast, colorectal, and ovarian cancer patients

The clinicopathological information for 57 patients with chemoresistant breast, colorectal, and ovarian cancer has been summarized in Table 1. Among 28 breast cancer patients who exhibited therapeutic resistance, the mean age was 50.29 ± 13.35 years. Notably, around 92.86 % of these patients were diagnosed with infiltrating ductal carcinoma. Most of the breast cancer patients (88.89 %) showed moderate cell differentiation (grade II).The mean age was 35.24 ± 11.56 years and 61.90 % were male patients among the 21 colorectal cancer patients. All the individuals had a diagnosis of colorectal adenocarcinoma. While half of the patients exhibited well-differentiated tissues, 40.00 % demonstrated moderate differentiation. There were eight ovarian cancer patients in this study with 87.50 % having papillary serous carcinoma and 12.50 % having squamous cell carcinoma. The average age of the patients was 53.13 ± 11.52 years. Almost 87.50 % of patients demonstrated poor differentiation (grade III) of tumor tissues.

3.2. Expression of HIF1A in chemoresistant breast, colorectal, and ovarian cancer

Significant alterations in HIF1A expression were observed between chemoresistant cancer tissues and corresponding control tissues across all three cancer types as illustrated in Fig. 1. In all three cancer types, a significant upregulation in the expression of HIF1A was documented in this study. The maximum level of elevation in the level of HIF1A expression was found in chemoresistant breast cancer tissues where the mean relative expression of HIF1A was almost nine-fold higher in chemoresistant cancer tissues compared to the paired control tissues (16.26 % vs. 1.88 %). This difference was found to be statistically significant (P value < 0.0001). For chemoresistant colorectal cancer tissues, the level of HIF1A overexpression was the lowest among the three cancer types. The average percentage of HIF1A expression was approximately 21.48 % in chemoresistant colorectal cancer tissues, nearly four-fold greater than the controls (5.54 %) (P value < 0.0001). Furthermore, the relative HIF1A expression in ovarian chemoresistant tissues was 21.93 %, whereas in controls that was 3.91 %, indicating a substantial and statistically significant change (P value $= 0.0020$). However, further analyses revealed that no significant associations existed between HIF1A expression in chemoresistant cancer tissues and the clinical data of the cancer patients.

3.3. Co-expression of ABC transporters and HIF1A in chemoresistant breast, colorectal, and ovarian cancer

3.3.1. ABC transporters and HIF1A co-expression in chemoresistant breast cancer

Concurrent expression of HIF1A and three ABC transporters (P-GP, MRP1, and BCRP) was observed in chemoresistant breast cancer tissue as illustrated in Fig. 2A. In contrast, such co-expression patterns were less pronounced and even absent in some cases in non-cancerous breast tissues (Fig. 2B).

Linear associations between the expression levels of HIF1A and ABC efflux transporters P-GP, MRP1, and BCRP in chemoresistance breast cancer and normal breast tissues are depicted in Fig. 2C, 2D, and 2E respectively. In case of all three ABC transporters, an elevation in the level of HIF1A coincided with an increase in the expression of transporter proteins. Among these three transporters, BCRP exhibited the highest amount of increase (1.08 unit) in response to a one-unit rise in HIF1A expression (Fig. 2E). Similarly, a one-unit increase in HIF1A expression corresponded to a 0.35 unit rise in P-GP (95 % CI: 0.19–0.51) and a 0.78 unit increase in MRP1 expression (95 % CI: 0.63–0.93) respectively (Fig. 2C and 2D). The positive linear correlation between these three ABC transporters and HIF1A was statistically significant as well.

The comparative co-expression patterns between ABC transporters (P-GP, MRP1, and BCRP) and HIF1A across chemoresistant breast cancer and paired control tissues have been depicted in Fig. 2F. In the case of all three transporters, a substantial increase in HIF1A-ABC transporter was observed in chemoresistant breast cancer tissues compared to paired control tissues. Among these three transporters, the co-expression of BCRP and HIF1A was the lowest in control tissues, however, the greatest level of elevation (~15-fold increase; 3.35 % vs 51.15 %) in co-expression with HIF1A was documented for BCRP in chemoresistant cancer tissues. For P-GP and HIF1A co-expression, the mean relative percentage in chemoresistant cancer tissues was 60.90 %, 10 times increase in expression compared to the controls (6.07 %) (P value $<$ 0.0001). Similarly, the co-expression of MRP1 and HIF1A increased from 7.04 % in control tissues to 63.18 % in chemoresistant breast cancer tissues, documenting an almost 9-fold increase in expression. In chemoresistant breast cancer tissues, MRP1 exhibited the highest level of co-expression with HIF1A among the three ABC transporters which was closely followed by P-GP. In addition, statistical analyses revealed the absence of any significant associations between ABC transporter-HIF1A co-expression with breast cancer patient data (Supplementary table 10).

3.3.2. ABC transporters and HIF1A co-expression in chemoresistant colorectal cancer

Chemoresistant colorectal cancer cells exhibit a significant level of co-expression between the three ABC transporters and HIF1A compared to control samples (Fig. 3A and 3B). The level of co-expression, as well as individual expression of these proteins, is much lower in control tissues than in chemoresistant tissues.

The linear correlation of separate expressions between ABC drug transporters and HIF1A in colorectal tissues revealed that upregulation in HIF1A expression was concomitant with a simultaneous increase in the expression of all three transporter proteins for colorectal tissues (Fig. 3C, 3D, and 3E). The magnitude of elevation in the level of BCRP was the highest among the three transporters in response to a rise in the HIF1A expression level. One-fold increase in HIF1A corresponded to a notable 1.75 unit increase in BCRP, with a statistically significant P value of < 0.0001 (Fig. 3E). In a similar manner, 1.08 unit and 1.17-unit elevation were observed in the level of P-GP and MRP1 respectively due to a singular unit rise in the level of HIF1A expression (Fig. 3C and 3D).

Variations in the co-expression pattern between the ABC transporters (P-GP, MRP1, and BCRP) and HIF1A in tissues obtained from chemoresistant and paired control samples of colorectal cancer patients are illustrated in Fig. 3F. Even though an increasing level of co-expression with HIF1A was observed for all three transporter proteins, the most substantial upregulation was observed for P-GP (Fig. 3F).The mean relative percentage observed in chemoresistant colorectal cancer tissues was 83.24 % for P-GP and HIF1A co-expression, approximately 2.5-fold higher than in controls (33.12 %) (P value < 0.0001). In the context of MRP1 and HIF1A co-expression, the relative percentage documented a two-fold increase, from 38.24 % in control tissues to 78.12 % in chemoresistant colorectal cancer tissues. In addition, the mean relative percentage of co-expression between BCRP and HIF1A in colorectal cancer chemoresistant tissues was 37.92 %, while it was 22.41 % in adjacent controls (P value < 0.0001). In chemoresistant colorectal cancer tissues, the level of concurrent expression between P-GP and HIF1A was the greatest, however, in control tissue the highest level of co-expression was observed for MRP1 and HIF1A, implying a greater role for P-GP in conferring drug resistance phenotype to colorectal cancer cells.

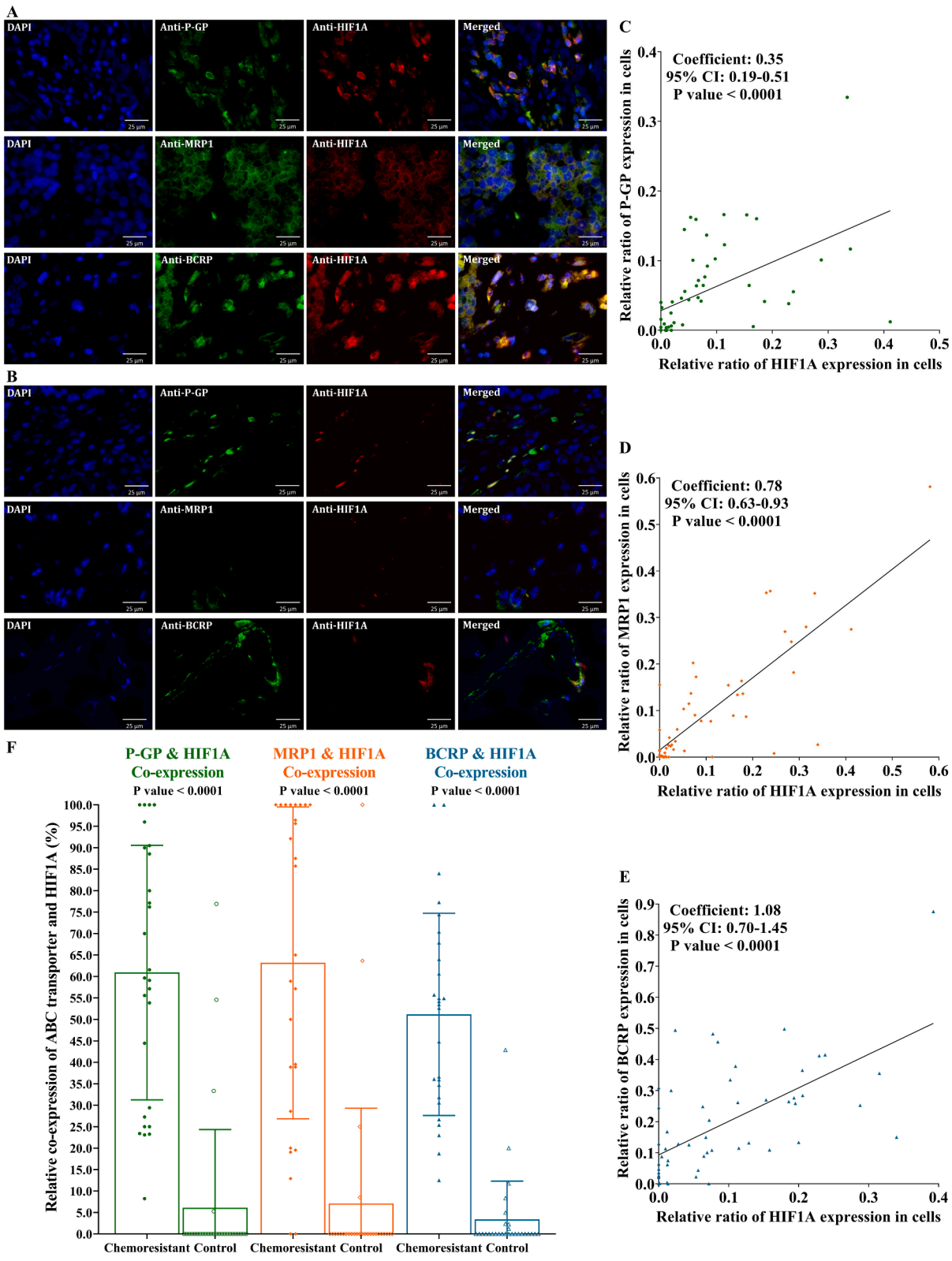

Fig. 2. ABC transporter and HIF1A co-expression profiles in chemoresistant cancerous and paired control breast tissues. (A) ABC transporters and HIF1A co-expression in chemoresistant breast cancer tissue. (B) ABC transporter and HIF1A co-expression in adjacent control tissues. In (A) and (B) the expressions of P-GP, MRP1, and BCRP are shown in green and HIF1A in red, respectively. The scale bar is 25 μm. (C), (D) and (E) show the correlations of P-GP, MRP1 and BCRP expressions with HIF1A, respectively, in breast tissues. The X-axis in (C), (D), and (E) denotes the relative ratio of HIF1A expression to total cells, whereas the Y-axis denotes the relative ratio of P-GP, MRP1, and BCRP expression in total cells, respectively. The slopes indicate linear relationship between transporters and HIF1A expression. (F) Comparison of ABC transporters and HIF1A co-expression in chemoresistant breast cancer and adjacent control tissues. The X-axis represents P-GP and HIF1A (green), MRP1 and HIF1A (orange), as well as BCRP and HIF1A (blue) co-expressions. The Y-axis denotes the relative percentage of ABC transporter and HIF1A co-expression. The Wilcoxon signed-rank test for paired samples was conducted to validate the significance of differences for all types of co-expression. (For interpretation of the references to colour in this figure legend, the reader is referred to the web version of this article.)

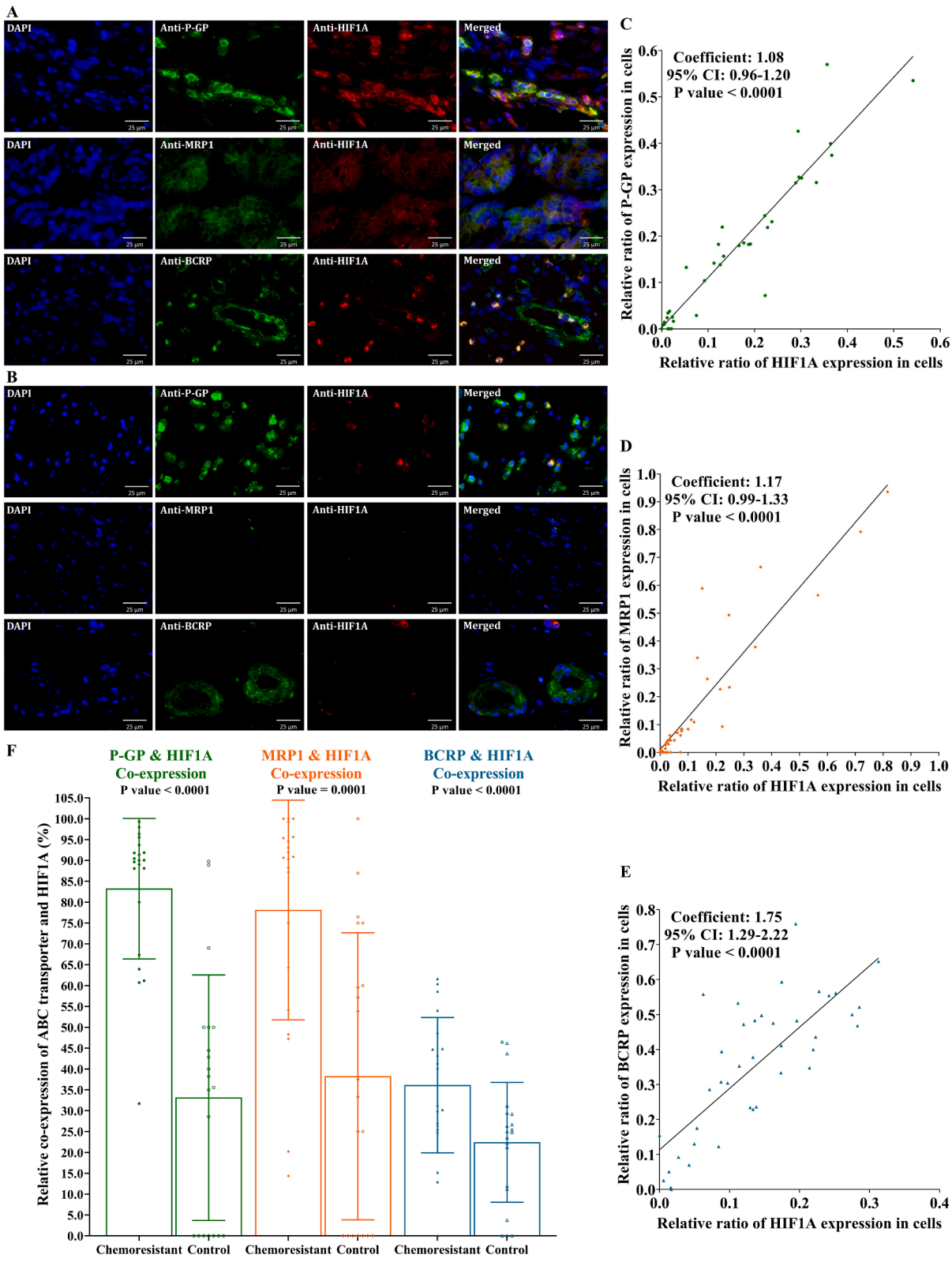

Fig. 3. ABC transporter and HIF1A co-expression profiles in chemoresistant cancerous and paired control colorectal tissues. (A) ABC transporters and HIF1A co-expression in chemoresistant colorectal cancer tissues. (B) ABC transporters and HIF1A co-expression in adjacent control tissues. In (A) and (B) the expressions of P-GP, MRP1, and BCRP are shown in green and HIF1A in red, respectively. The scale bar is 25 μm. (C), (D) and (E) show the correlations of P-GP, MRP1 and BCRP expressions with HIF1A, respectively, in colorectal tissues. The X-axis in (C), (D), and (E) denotes the relative ratio of HIF1A expression to total cells. The Y-axis in (C), (D), and (E) denotes the relative ratio of P-GP, MRP1, and BCRP expression to total cells, respectively. The slopes indicate the linear relationship between transporters and HIF1A expression. (F) Comparison of ABC transporter and HIF1A co-expression in chemoresistant colorectal cancer and adjacent control tissues. The X-axis represents P-GP and HIF1A (green), MRP1 and HIF1A (orange), and BCRP and HIF1A (blue) co-expressions. The Y-axis denotes the relative percentage of ABC transporter and HIF1A co-expression. The Wilcoxon signed-rank test for paired samples was conducted to validate the significance of differences for all types of co-expression. (For interpretation of the references to colour in this figure legend, the reader is referred to the web version of this article.)

Among chemoresistant colorectal cancer patients, the differentiation of cells and cancer grade was significantly correlated with P-GP and HIF1A co-expression (P value = 0.047) (Supplementary table 11). In Grade II and moderately differentiated colorectal cancer tissues, P-GP and HIF1A co-expression was the highest (0.91 ± 0.10) while in poorly differentiated grade III tumors, the co-expression level was the lowest.

3.3.3. ABC transporters and HIF1A co-expression in chemoresistant ovarian cancer

Immunostained chemoresistant ovarian cancer cells demonstrate quite a substantial level of co-expression of HIF1A with all three ABC transporters (P-GP, MRP1, and BCRP) in comparison with adjacent control tissues as illustrated in Fig. 4A and 4B.

The linear regression models suggest positive linear associations between ABC drug transporters and HIF1A individual expressions in the ovary (Fig. 4C, 4D, and 4E). Interestingly, like in breast and colorectal cancers, elevation in the relative expression of all transporter proteins was observed in conjunction with an increasing HIF1A expression. Unlike the previous two cancers, the most substantial level of elevation (1.24-unit increase) was observed for P-GP due to a single unit rise in the level of HIF1A expression (Fig. 4C). Similarly, a single unit elevation of HIF1A corresponded to a 1.09-unit upregulation in the expression of MRP1 (95 % CI: 1.04–1.14) and a slightly lower 0.96 unit increase in BCRP expression (95 % CI: 0.55–1.38) (P value = 0.0002) (Fig. 4D and 4E).

A comparative analysis of ABC transporters and HIF1A co-expression between chemoresistant ovarian cancer and control tissues has been depicted in Fig. 4F. In the case of all three transporters, significant upregulation of co-expression with HIF1A was observed. The magnitude of co-expression was the highest for MRP1 and HIF1A in chemoresistant tissue of ovarian cancer. Nevertheless, the greatest level of increase in co-expression with HIF1A was documented for BCRP, more than two times elevation in chemoresistant ovarian cancer tissues compared to control tissues. In the context of P-GP and HIF1A relative co-expression, the mean percentages in chemoresistant and control tissues were 84.66 % and 55.85 %, respectively (P value = 0.0156). The relative average percentage in chemoresistant ovarian cancer tissues was 92.40 % for MRP1 and HIF1A co-expression, whereas the percentage was approximately half (58.47 %) in controls (P value = 0.0313). In addition, statistical analyses also indicated that there was not any significant association between ovarian cancer patient information and ABC drug transporter and HIF1A co-expression (Supplementary table 12).

3.3.4. 3D modeling of HIF1A protein and its target binding site and molecular docking between them

The predicted 3D structure of the HIF1A protein is presented as Supplementary Fig. 3A. Quality assessment of the predicted 3D structure of the protein revealed the model to be acceptable for further analysis (Supplementary Fig. 3B, 3C, and 3D). From the Ramachandran plot, it was observed that a total of 98.10 %{most favored region (91.60 %) + additional allowed region (6.20 %) + generally allowed region (0.30 %)} of the AA residues were in the allowed region (Supplementary Fig. 3B).

The HRE regions were −1345 to −1349 for *ABCB1*, −1518 to −1522 for *ABCC1*, and −10432 to −10436 for *ABCG2* (Supplementary Fig. 4). 3D DNA models were generated from these identified stretches of DNA.

We next modeled the interactions between HIF1A protein and HRE in the promoter regions of the ABC transporter genes which is illustrated in Fig. 5. All the Z-scores found from docking were negative which was indicative of stable binding of the HIF1A protein to the HRE regions of promoter element. Additionally, other comprehensive information such as the Haddock score, cluster size, RMSD from the overall lowest-energy structure, Van der Waals energy, electrostatic energy, desolvation energy, restraints violation energy, and buried surface area for all dockings are provided in Supplementary table 13.

4. Discussion

Chemoresistance poses one of the most significant challenges in the treatment of advanced cancer patients undergoing chemotherapy as it leads to treatment failure and diminishes the survival rate in cancer patients.[65] Among all mechanisms, reduced intracellular accumulation of drugs is considered a prominent contributor to the development of anti-cancer drug resistance.[66]Many membrane transporters facilitate the decrease in drug accumulation inside cells, thereby conferring resistance to commonly employed chemotherapeutic agents.[67] ABC transporters are the most prominent transmembrane protein group in actively extruding various structurally and mechanistically distinct chemotherapeutic agents outside cells.[68] While this protein superfamily comprises 49 members, only three – P-GP, MRP1, and BCRP– have been extensively implicated in multidrug resistance.[4,69]

HIF1A, a master regulator of transcriptional activity, is induced in response to hypoxic conditions and its elevated expression has been linked to various aspects of cancer cells including metabolism, angiogenesis, invasion as well as therapeutic resistance.[43–44] Besides, it has been implicated in the development of therapeutic resistance in a variety of cancers including breast cancer, gastric cancer, etc.[70,71] ABC transporters like P-GP and MRP1 were found to be hypoxia-responsive and so regulated by HIF1A.[50,53] However, the precise role and function of HIF1A in the ABC transporter-mediated chemoresistance mechanism as well as the dynamics of concurrent expression of HIF1A with the three ABC transporters remain largely mysterious. Therefore, this study employed a variety of experimental and computational techniques to determine the dynamics and pattern of co-expression between HIF1A and each of the three ABC transporters (P-GP, MRP1, and BCRP) in chemoresistant breast, colorectal, and ovarian cancers.

Enhanced expression of HIF1A is a key feature in most malignancies as the tumor-microenvironment is primarily hypoxic in nature.[43,72,73] Additionally, hypoxic cells where HIF1A expression has been induced demonstrate increased resistance to chemotherapy.[74] Therefore, the expression level of HIF1A was compared between chemoresistant cancer tissues and adjacent control tissues to identify any changes in the level of this transcription regulatory protein. Immunostaining of HIF1A revealed a substantial elevation in the HIF1A protein level in chemoresistant tissues across all three cancers (breast, colorectal, and ovarian cancer). Among control breast, colorectal, and ovarian tissues, the greatest level of expression of HIF1A was documented in the normal colorectal tissues. However, in the case of chemoresistant tissues, HIF1A expression in ovarian tissues superseded that of colorectal tissues implying a far greater role of HIF1A in inducing drug-resistant phenotype in the ovarian tissues. Despite the greater level of HIF1A in chemoresistant ovarian tissues compared to the other two tissue types, the most substantial level of increase, almost nine-fold in magnitude, was observed for chemoresistant breast cancer tissues compared to paired control tissues. This particular outcome of this study implies a key role for HIF1A in driving therapeutic resistance in breast cancer. This finding is well supported by the results of earlier studies where HIF1A has been found to have a pleiotropic role in conferring therapeutic resistance to breast cancer tissues.[70,75,76] Besides, it was observed that the co-expression pattern of HIF1A and ABC transporters aligned with HIF1A expression alone in breast, colorectal, and ovarian tissues. Both the expression of HIF1A alone and the HIF1A-ABC co-expression were more elevated in colorectal and ovarian tissues than in breast tissues.

When the extent of co-expression between P-GP and HIF1A was investigated in this study, it was found that there exists a significant correlation between the expression of P-GP and HIF1A across all three cancer types. The linear regression relationship between the expression of P-GP and HIF1A was more pronounced in ovarian cancer than the other two cancers as indicated by a greater magnitude of co-efficient (Fig. 2C, 3C, and 4C). This indicates a greater role of HIF1A in chemoresistant ovarian tissues in inducing the overexpression of P-GP. In terms of the changes in co-expression due to the acquisition of resistance

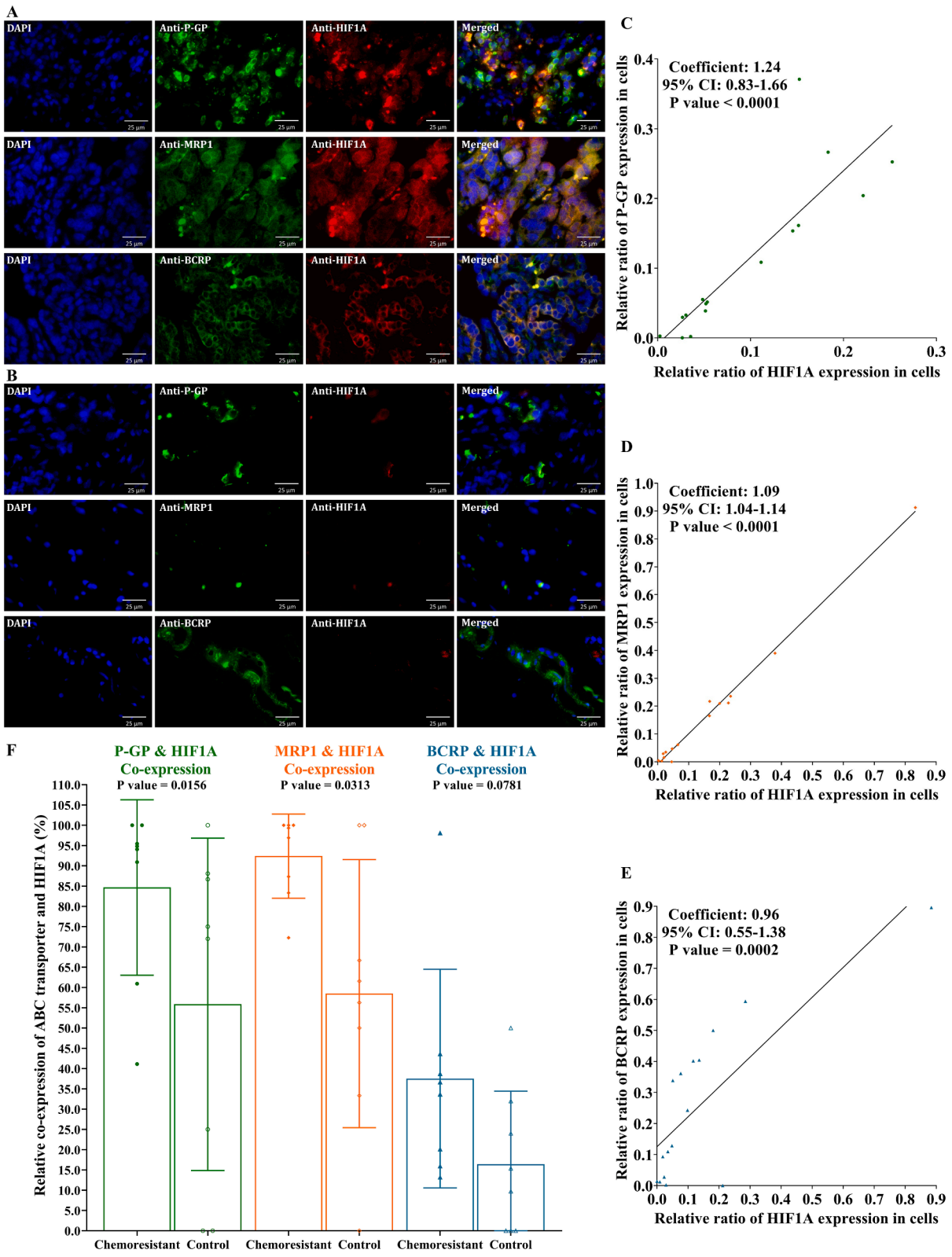

Fig. 4. ABC transporter and HIF1A co-expression profiles in chemoresistant cancerous and paired control ovarian tissues. (A) ABC transporters and HIF1A co-expression in chemoresistant ovarian cancer tissues. (B) ABC transporters and HIF1A co-expression in adjacent control tissues. In (A) and (B) the expressions of P-GP, MRP1, and BCRP are shown in green and HIF1A in red, respectively. The scale bar is 25 μm. (C), (D) and (E) show the correlations of P-GP, MRP1 and BCRP expressions with HIF1A, respectively, in colorectal tissues in ovarian tissues. The X-axis in (C), (D), and (E) denotes the relative ratio of HIF1A expression to total cells. The Y-axis in (C), (D), and (E) denotes the relative ratio of P-GP, MRP1, and BCRP expression to total cells, respectively. The slopes indicate the linear relationship between transporters and HIF1A expression. (F) Comparison of ABC transporter and HIF1A co-expression in chemoresistant ovarian cancer and adjacent control tissues. The X-axis represents P-GP and HIF1A (green), MRP1 and HIF1A (orange), and BCRP and HIF1A (blue) co-expressions. The Y-axis denotes the relative percentage of ABC transporter and HIF1A co-expression. The Wilcoxon signed-rank test for paired samples was conducted to validate the significance of differences for all types of co-expression. (For interpretation of the references to colour in this figure legend, the reader is referred to the web version of this article.)

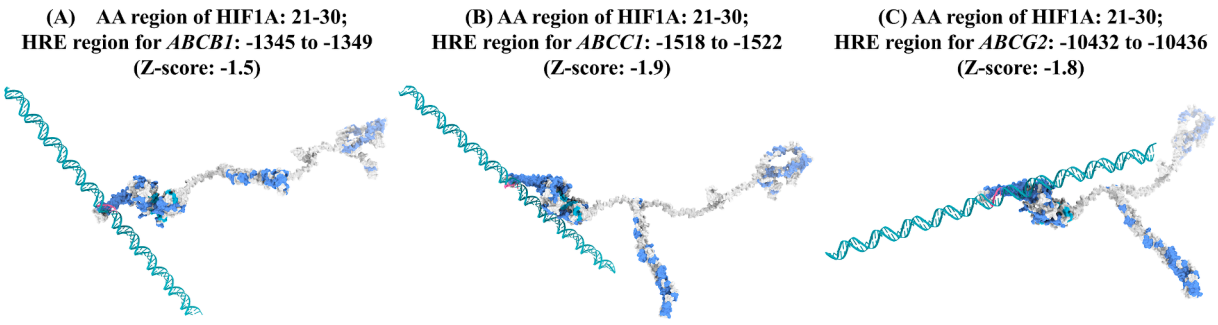

Fig. 5. Molecular docking of HIF1A with HRE sequence of ABC transporter gene promoter regions. (A) Docking of HIF1A (AA region: 21–30) and *ABCB1* gene promoter region (Z-score: −1.5). (B) Representative docking of HIF1A (AA region: 21–30) and *ABCC1* gene promoter region (Z-score: −1.9). (C) Representative docking of HIF1A (AA region: 21–30) and *ABCG2* gene promoter region (Z-score: −1.8).

properties, the greatest level of elevation in the concurrent expression of P-GP and HIF1A was documented in chemoresistant breast cancer tissue, approximately 10-fold higher compared to paired control tissues (Fig. 2F). Similarly, co-expression of P-GP and HIF1A was upregulated in both chemoresistant colorectal and ovarian tissues, by a magnitude of 2.5 times and 1.5 times respectively (Fig. 3F, and 4F).These findings are aligned with some previous research. Under hypoxic conditions, both HIF1A and *ABCB1* mRNAs exhibit a substantial rise compared to normoxia across the same cell populations.[77] On the other hand, the HIF1A protein was also found to be binding to the *ABCB1* gene's promoter under normoxic conditions.[49] Another study reported the hypoxia responsiveness of the *ABCB1* gene.[50] Moreover, overexpression of HIPK2 has been observed to diminish HIF1 transcriptional activity which resulted in P-GP abolition, and adverse drug reaction-induced apoptosis.[51] All these results together indicate a significant role of HIF1A in inducing the overexpression of P-GP in chemoresistant cancer cells of breast, colorectal, and ovarian origin.

This study also demonstrated that the extent of co-expression between P-GP and HIF1A is substantially correlated with the differentiation of tumor tissues as well as the grade of the tumor. The co-expression level was elevated in moderately differentiated grade II tumors compared to well-differentiated grade I tumors which is indicative of a role for both P-GP and MRP1 in the progression of cancer from a well-differentiated tissue histology to a moderately differentiated one.

Quite like P-GP and HIF1A co-expression, MRP1 and HIF1A also exhibited higher co-expression levels across all three chemoresistant cancer tissues, which was about 9 folds higher in the breast tissues, 2-fold higher in the colorectal tissues, and 1.6-fold higher in the ovarian tissues (Fig. 2F, 3F, and 4F). In addition, a significant level of linear dependency was observed between the expression of MRP1 and HIF1A. Such findings imply a role for HIF1A in modulating the expression of MRP1 in the chemoresistant breast, colorectal, and ovarian cancer tissues. The correlation between the level of HIF1A and MRP1 was quite similar in colorectal and ovarian tissues (1.17 and 1.09 respectively) while it was the lowest for breast tissues indicating a more profound role of HIF1A in the upregulation of MRP1 in both ovarian and colorectal tissues (Fig. 2D, 3D, and 4D).Like P-GP, MRP1 was also documented as a drug-resistance protein associated with hypoxia.[78–79] Besides, inhibition of HIF1A through siRNA and dominant-negative HIF1A has been demonstrated to drive MRP1 expression down.[80] Furthermore, a study by Chen et al. demonstrated that HIF1A suppression can decrease MRP1-regulated drug resistance in lung and liver carcinomas.[49]

In the case of co-expression of BCRP and HIF1A in chemoresistant breast cancer and colorectal cancer, the overexpression followed the same trend as P-GP and HIF1A, as well as MRP1 and HIF1A co-expressions. Throughout the drug-resistant cancer tissues, the co-expression levels were 15.3- (breast cancer) and 1.7-fold (colorectal cancer) higher than the adjacent control tissues (Fig. 2F and 3F). In addition, statistically significant linear relations between HIF1A and BCRP expression was documented across all three cancer tissues inferring the involvement of HIF1A in inducing BCRP expression in those tissues via modulating transcriptional activity (Fig. 2E, 3E, and 4E). The coefficient for the linear relation between HIF1A and BCRP was the greatest for colorectal tissues which implies a far greater role for HIF1A in inducing BCRP-mediated therapeutic resistance in colorectal cancer (Fig. 3E). This relation of HIF1A regulating the transcription of *ABCG2* mRNA was first addressed by Krishnamurthy *et al.* in 2004.[81] They reported that HIF1A binds with the HRE in the BCRP promoter region under hypoxic conditions. Another research revealed that activation of HIF1A stimulates the ERK1/2/HIF1A axis that translocate the BCRP efflux pump from the cytoplasm to the cell membrane.[82]

As our experimental findings suggested that concurrent upregulation of HIF1A and ABC transporters facilitate the development of therapeutic resistance, *in silico* experiments were performed to predict the binding of HIF1A to the promoter region of these three transporters' genes. By binding to the HRE of the promoter sequence of a gene, HIF1A exerts its influence on transcription induction. Through bioinformatic analysis, the HRE sequences were found within −2000 bp before the 5′ end for *ABCB1* and *ABCC1*, whereas −10432 bp for BCRP, respectively. Molecular docking analyses of these regions with HIF1A helped us discern their binding capabilities. Interestingly, all the Z-scores derived from the docking experiments were highly negative (Supplementary Table 13), supporting the hypothesis that HIF1A potentially stimulates the transcription of all three selected ABC transporters via binding to this region.

By examining the molecular docking analyses, the linear associations of individual expressions, and the co-expression patterns between the three ABC transporters and HIF1A, we propose that HIF1A directly regulates the transcription of key efflux pumps (P-GP, MRP1, and BCRP) possibly by binding to the HRE sequence upstream the promoter regions of their respective genes. Interestingly, P-GP and MRP1 demonstrated almost comparable co-expression levels with HIF1A, surpassing that of BCRP. This discrepancy may be attributed to the proximity of the HRE sequence in the promoter regions, situated within 1345 bp for *ABCB1* and 1518 bp for *ABCC1*, while ranging to 10432 bp for *ABCG2*. The findings of this study also suggest that HIF1A could enhance the transcription of all three transporters concurrently for the same patients, potentially leading to the emergence of therapeutic resistance and poorer prognosis. Therefore, inhibition of HIF1A from binding to the HRE region of ABC efflux pumps' promoters could drastically reverse chemoresistance mechanisms and improve the likelihood of favorable clinical outcomes in cancer patients.

Limitations of the study: Despite several strengths, there are some limitations of this study. As the objective was to explore the correlation of HIF1A and the ABC transporter expression profiles in chemoresistant cancer cells, we did not include treatment regimen related data. Moreover, due to limited resources and challenges in sample collection, we were unable to incorporate additional techniques such as knockdown models, qPCR, western blot, drug sensitivity assays, etc.

5. Conclusion

In the pursuit of bridging a crucial gap in research on cancer chemoresistance, this study aimed to elucidate the intricate mechanisms behind therapeutic resistance in breast, colorectal, and ovarian cancer. This investigation focused on the co-expression associations of key proteins (P-GP, MRP1, BCRP, and HIF1A) in chemoresistant tissues obtained from Bangladeshi cancer patients. The observed overexpression of HIF1A in chemoresistant tissues implicates their pivotal roles behind resistance mechanisms across various malignancies. HIF1A directly regulates the transcription of key efflux pumps by binding to the HRE sequence in their promoter regions. Inhibition of HIF1A to these promoter regions may appear as a promising avenue for overcoming chemoresistance. Even though a larger sample size, as well as experimental techniques like western blotting, immunoprecipitation, and knockout studies, would provide useful information, this study particularly serves as a stepping stone for future research in addressing the phenomenon of HIF1A-driven chemoresistance in cancer.

Ethical approval

This study was approved by the Ethics Review Committee of the Faculty of Biological Sciences at the University of Dhaka (117/Biol.Scs).

Funding source

This study was supported by the Centennial Research Grant from the University of Dhaka to AAS. The authors are thankful for the support.

CRediT authorship contribution statement

Sudipta Deb Nath: Writing – original draft, Validation, Methodology, Investigation. **Md Tamzid Hossain Tanim:** Writing – review & editing, Data curation. **Mahmudul Hasan Akash:** Validation, Methodology, Investigation. **Mohammad Golam Mostafa:** Writing – review & editing, Resources. **Abu Ashfaqur Sajib:** Conceptualization, Funding acquisition, Project administration, Writing – review & editing, Supervision, Resources.

Declaration of competing interest

The authors declare that they have no known competing financial interests or personal relationships that could have appeared to influence the work reported in this paper.

Acknowledgements

This study was supported by the Centennial Research Grant from the University of Dhaka, Bangladesh to AAS. The authors are thankful for the support.

Appendix A. Supplementary data

Supplementary data to this article can be found online at https://doi.org/10.1016/j.jgeb.2025.100496.

References

1. Rich JN, Bao S. Chemotherapy and cancer stem cells. *Cell Stem Cell*. 2007;1:353–355. https://doi.org/10.1016/j.stem.2007.09.011.
2. Szakács G, Paterson JK, Ludwig JA, Booth-Genthe C, Gottesman MM. Targeting multidrug resistance in cancer. *Nat Rev Drug Discov*. 2006;5:219–234. https://doi.org/10.1038/nrd1984.
3. Nath SD, Shoily SS, Fatema K, Khan A, Mostafa MG, Sajib AA. Pan-cancer chemoresistance-associated genes, affected pathways and potential therapeutic targets. *Human Gene*. 2023;35. https://doi.org/10.1016/j.humgen.2023.201151.
4. Gottesman MM, Fojo T, Bates SE. Multidrug resistance in cancer: Role of ATP-dependent transporters. *Nat Rev Cancer*. 2002;2:48–58. https://doi.org/10.1038/nrc706.
5. Corrie PG. Cytotoxic chemotherapy: clinical aspects. *Medicine*. 2008;36:24–28. https://doi.org/10.1016/j.mpmed.2007.10.012.
6. Longley DB, Johnston PG. Molecular mechanisms of drug resistance. *J Pathol*. 2005;205:275–292. https://doi.org/10.1002/path.1706.
7. Andersen MH, Sørensen RB, Schrama D, Svane IM, Becker JC, Thor SP. Cancer treatment: the combination of vaccination with other therapies. *Cancer Immunol Immunother*. 2008;57:1735–1743. https://doi.org/10.1007/s00262-008-0480-y.
8. Martin HL, Smith L, Tomlinson DC. Multidrug-resistant breast cancer: current perspectives. *Breast Cancer: Targets and Therapy*. 2014;6:1–13. https://doi.org/10.2147/BCTT.S37638.
9. War AR. Curcumin co-treatment sensitizes multi-drug resistant Ht29 colon cancer cell line. *Journal of Cancer Research and Immuno-Oncology*. 2018;04. https://doi.org/10.35248/2684-1266.18.4.117.
10. Kim H, Kim K, No JH, Jeon YT, Jeon HW, Kim YB. Prognostic value of biomarkers related to drug resistance in patients with advanced epithelial ovarian cancer. *Anticancer Res*. 2012;32:589–594.
11. Zong L, Pi Z, Liu S, Liu Z, Song F. Metabolomics analysis of multidrug-resistant breast cancer cells: In vitro using methyl- tert -butyl ether method. *RSC Adv*. 2018;8:15831–15841. https://doi.org/10.1039/c7ra12952a.
12. Yuan Z, Shi X, Qiu Y, et al. Reversal of P-gp-mediated multidrug resistance in colon cancer by cinobufagin. *Oncol Rep*. 2017;37:1815–1825. https://doi.org/10.3892/or.2017.5410.
13. Ye Q, Liu K, Shen Q, et al. Reversal of multidrug resistance in cancer by multi-functional flavonoids. *Front Oncol*. 2019;9. https://doi.org/10.3389/fonc.2019.00487.
14. Ueda K, Cardarelli C, Gottesman MM, Pastan T. Expression of a full-length cDNA for the human "MDR1" gene confers resistance to colchicine, doxorubicin, and vinblastine. *Proc Natl Acad Sci U S A*. 1987;84:3004–3008. https://doi.org/10.1073/pnas.84.9.3004.
15. Robinson K, Tiriveedhi V. Perplexing Role of P-Glycoprotein in Tumor Microenvironment. *Front Oncol*. 2020;10:265. https://doi.org/10.3389/fonc.2020.00265.
16. Mo W, Zhang JT. Human ABCG2: Structure, function, and its role in multidrug resistance. Int J Biochem Mol Biol 2012;3.
17. Polgar O, Robey RW, Bates SE. ABCG2: Structure, function and role in drug response. *Expert Opin Drug MetabToxicol*. 2008;4:1–15. https://doi.org/10.1517/17425255.4.1.1.
18. Kachalaki S, Ebrahimi M, Mohamed Khosroshahi L, Mohammadinejad S, Baradaran B. Cancer chemoresistance; biochemical and molecular aspects: a brief overview. *Eur J Pharm Sci*. 2016;89:20–30. https://doi.org/10.1016/j.ejps.2016.03.025.
19. Lu JF, Pokharel D, Bebawy M. MRP1 and its role in anticancer drug resistance. *Drug Metab Rev*. 2015;47:406–419. https://doi.org/10.3109/03602532.2015.1105253.
20. Ni Z, Bikadi Z, F. Rosenberg M, Mao Q. Structure and Function of the Human Breast Cancer Resistance Protein (BCRP/ABCG2). Curr Drug Metab 2010;11:603–17. doi: 10.2174/138920010792927325.
21. Slot AJ, Molinski SV, Cole SPC. Mammalian multidrug-resistance proteins (MRPs). *Essays Biochem*. 2011;50:179–207. https://doi.org/10.1042/BSE0500179.
22. Zhou S-F, Wang L-L, Di Y, et al. Substrates and inhibitors of human multidrug resistance associated proteins and the implications in drug development. *Curr Med Chem*. 2008;15:1981–2039. https://doi.org/10.2174/092986708785132870.
23. Koh EH, Chung HC, Lee KB, et al. The value of immunohistochemical detection of P-glycoprotein in breast cancer before and after induction chemotherapy. *Yonsei Med J*. 1992;33:137–142. https://doi.org/10.3349/ymj.1992.33.2.137.
24. Mechetner E, Kyshtoobayeva A, Zonis S, et al. Levels of multidrug resistance (MDR1) P-glycoprotein expression by human breast cancer correlate with in vitro resistance to taxol and doxorubicin. *Clin Cancer Res*. 1998;4:389–398.
25. Penson RT, Oliva E, Skates SJ, et al. Expression of multidrug resistance-1 protein inversely correlates with paclitaxel response and survival in ovarian cancer patients: a study in serial samples. *Gynecol Oncol*. 2004;93:98–106. https://doi.org/10.1016/j.ygyno.2003.11.053.
26. Baekelandt MM, Holm R, Nesland JM, Tropé CG, Kristensen GB. P-glycoprotein expression is a marker for chemotherapy resistance and prognosis in advanced ovarian cancer. *Anticancer Res*. 2000;20:1061–1067.
27. Linn SC, Giaccone G. MDR1/P-glycoprotein expression in colorectal cancer. *Eur J Cancer*. 1995;31:1291–1294. https://doi.org/10.1016/0959-8049(95)00278-Q.
28. Leonard GD, Fojo T, Bates SE. The role of ABC transporters in clinical practice. *Oncologist*. 2003;8:411–424. https://doi.org/10.1634/theoncologist.8-5-411.
29. Deeley RG, Westlake C, Cole SPC. Transmembrane transport of endo- and xenobiotics by mammalian ATP-binding cassette multidrug resistance proteins. *Physiol Rev*. 2006;86:849–899. https://doi.org/10.1152/physrev.00035.2005.
30. Nakanishi T, Chumsri S, Khakpour N, et al. Side-population cells in luminal-type breast cancer have tumour-initiating cell properties, and are regulated by HER2 expression and signalling. *Br J Cancer*. 2010;102:815–826. https://doi.org/10.1038/sj.bjc.6605553.
31. Fang DD, Kim YJ, Lee CN, et al. Expansion of CD133+ colon cancer cultures retaining stem cell properties to enable cancer stem cell target discovery. *Br J Cancer*. 2010;102:1265–1275. https://doi.org/10.1038/sj.bjc.6605610.
32. Chikazawa N, Tanaka H, Tasaka T, et al. Inhibition of Wnt signaling pathway decreases chemotherapy-resistant side-population colon cancer cells. *Anticancer Res*. 2010;30:2041–2048.

33. Wang YH, Li F, Luo B, et al. A side population of cells from a human pancreatic carcinoma cell line harbors cancer stem cell characteristics. *Neoplasma*. 2009;56: 371–378. https://doi.org/10.4149/neo_2009_05_371.
34. Hu L, McArthur C, Jaffe RB. Ovarian cancer stem-like side-population cells are tumourigenic and chemoresistant. *Br J Cancer*. 2010;102:1276–1283. https://doi.org/10.1038/sj.bjc.6605626.
35. Liu T, Xu F, Du X, et al. Establishment and characterization of multi-drug resistant, prostate carcinoma-initiating stem-like cells from human prostate cancer cell lines 22RV1. *Mol Cell Biochem*. 2010;340:265–273. https://doi.org/10.1007/s11010-010-0426-5.
36. Ning ZF, Huang YJ, Lin TX, et al. Subpopulations of stem-like cells in side population cells from the human bladder transitional cell cancer cell line T24. *J Int Med Res*. 2009;37:621–630. https://doi.org/10.1177/147323000903700304.
37. Semenza GL. Regulation of mammalian O2 homeostasis by hypoxia-inducible factor 1. *Annu Rev Cell Dev Biol*. 1999;15:551–578. https://doi.org/10.1146/annurev.cellbio.15.1.551.
38. Semenza GL. HIF-1: mediator of physiological and pathophysiological responses to hypoxia. *J Appl Physiol*. 2000;88:1474–1480. https://doi.org/10.1152/jappl.2000.88.4.1474.
39. Jaakkola P, Mole DR, Tian YM, et al. Targeting of HIF-α to the von Hippel-Lindau ubiquitylation complex by O2-regulated prolyl hydroxylation. *Science*. 1979;2001 (292):468–472. https://doi.org/10.1126/science.1059796.
40. Iyer NV, Kotch LE, Agani F, et al. Cellular and developmental control of O2 homeostasis by hypoxia- inducible factor 1α. *Genes Dev*. 1998;12:149–162. https://doi.org/10.1101/gad.12.2.149.
41. Bateman A, Martin MJ, Orchard S, et al. UniProt: the Universal Protein Knowledgebase in 2023. *Nucleic Acids Res*. 2023;51:D523–D531. https://doi.org/10.1093/nar/gkac1052.
42. Wenger RH, Stiehl DP, Camenisch G. Integration of oxygen signaling at the consensus HRE. *Sci STKE 2005*. 2005. https://doi.org/10.1126/stke.3062005re12.
43. Semenza GL. Targeting HIF-1 for cancer therapy. *Nat Rev Cancer*. 2003;3:721–732. https://doi.org/10.1038/nrc1187.
44. Shan B, Gerez J, Haedo M, et al. RSUME is implicated in HIF-1-induced VEGF-A production in pituitary tumour cells. *EndocrRelat Cancer*. 2012;19:13–27. https://doi.org/10.1530/ERC-11-0211.
45. Lambert SA, Jolma A, Campitelli LF, et al. The human transcription factors. *Cell*. 2018;172:650–665. https://doi.org/10.1016/j.cell.2018.01.029.
46. Jia X, Hong Q, Lei L, et al. Basal and therapy-driven hypoxia-inducible factor-1α confers resistance to endocrine therapy in estrogen receptor-positive breast cancer. *Oncotarget*. 2015;6:8648–8662. https://doi.org/10.18632/oncotarget.3257.
47. Li M, Li L, Cheng X, Li L, Tu K. Hypoxia promotes the growth and metastasis of ovarian cancer cells by suppressing ferroptosis via upregulating SLC2A12. *Exp Cell Res*. 2023;433, 113851. https://doi.org/10.1016/j.yexcr.2023.113851.
48. Zhao Y, Xing C, Deng Y, Ye C, Peng H. HIF-1α signaling: essential roles in tumorigenesis and implications in targeted therapies. *Genes Dis*. 2024;11:234–251. https://doi.org/10.1016/j.gendis.2023.02.039.
49. Chen J, Ding Z, Peng Y, et al. HIF-1α inhibition reverses multidrug resistance in colon cancer cells via downregulation of MDR1/P-glycoprotein. *PLoS One*. 2014;9, e98882. https://doi.org/10.1371/journal.pone.0098882.
50. Comerford KM, Wallace TJ, Karhausen J, Louis NA, Montalto MC, Colgan SP. Hypoxia-inducible factor-1-dependent regulation of the multidrug resistance (MDR1) gene. *Cancer Res*. 2002;62:3387–3394.
51. Nardinocchi L, Puca R, Sacchi A, D'Orazi G. Inhibition of HIF-1alpha activity by homeodomain-interacting protein kinase-2 correlates with sensitization of chemoresistant cells to undergo apoptosis. *Mol Cancer*. 2009;8:1–9. https://doi.org/10.1186/1476-4598-8-1.
52. He X, Wang J, Wei W, et al. Hypoxia regulates ABCG2 activity through the activivation of ERK1/2/HIF-1α and contributes to chemoresistance in pancreatic cancer cells. *Cancer Biol Ther*. 2016;17:188–198. https://doi.org/10.1080/15384047.2016.1139228.
53. Lv Y, Zhao S, Han J, Zheng L, Yang Z, Zhao L. Hypoxia-inducible factor-1α induces multidrug resistance protein in colon cancer. *Onco Targets Ther*. 2015;8:1941–1948. https://doi.org/10.2147/OTT.S82835.
54. Diamond TM, Sutphen R, Tabano M, Fiorica J. Inherited susceptibility to breast and ovarian cancer. *Curr Opin Obstet Gynecol*. 1998;10. https://doi.org/10.1097/00001703-199802000-00002.
55. Tung KH, Goodman MT, Wu AH, et al. Aggregation of cancer with breast, ovarian, colorectal, and prostate cancer in first-degree relatives. *Am J Epidemiol*. 2004;159. https://doi.org/10.1093/aje/kwh103.
56. Rasband WS. ImageJ. U S National Institutes of Health, Bethesda, Maryland, USA, 1997-2018 n.d.
57. Ko J, Park H, Heo L, Seok C. GalaxyWEB server for protein structure prediction and refinement. *Nucleic Acids Res*. 2012;40:W294–W297. https://doi.org/10.1093/nar/gks493.
58. Laskowski RA, MacArthur MW, Thornton JM. PROCHECK : validation of protein-structure coordinates, 2012. doi: 10.1107/97809553602060000882.
59. Benkert P, Biasini M, Schwede T. Toward the estimation of the absolute quality of individual protein structure models. *Bioinformatics*. 2011;27:343–350. https://doi.org/10.1093/bioinformatics/btq662.
60. Wiederstein M, Sippl MJ. ProSA-web: Interactive web service for the recognition of errors in three-dimensional structures of proteins. *Nucleic Acids Res*. 2007;35: W407–W410. https://doi.org/10.1093/nar/gkm290.
61. Sayers EW, Bolton EE, Brister JR, et al. Database resources of the national center for biotechnology information. *Nucleic Acids Res*. 2022;50:D20–D26. https://doi.org/10.1093/nar/gkab1112.
62. Arnott S, Campbell-Smith PJ, Chandrasekaran R. In Handbook of Biochemistry and Molecular Biology. vol. II. 3rd ed. Cleveland: CRC Press; 1976.
63. Van Zundert GCP, Rodrigues JPGLM, Trellet M, et al. The HADDOCK2.2 web server: user-friendly integrative modeling of biomolecular complexes. *J Mol Biol*. 2016;428: 720–725. https://doi.org/10.1016/j.jmb.2015.09.014.
64. Pettersen EF, Goddard TD, Huang CC, et al. UCSF ChimeraX: structure visualization for researchers, educators, and developers. *Protein Sci*. 2021;30:70–82. https://doi.org/10.1002/pro.3943.
65. Hamilton G, Rath B. A short update on cancer chemoresistance. *Wiener MedizinischeWochenschrift*. 2014;164:456–460. https://doi.org/10.1007/s10354-014-0311-z.
66. McCarroll JA, Naim S, Sharbeen G, et al. Role of pancreatic stellate cells in chemoresistance in pancreatic cancer. *Front Physiol*. 2014;5:86505. https://doi.org/10.3389/fphys.2014.00141.
67. Wang X, He S, Gu Y, et al. Fatty acid receptor GPR120 promotes breast cancer chemoresistance by upregulating ABC transporters expression and fatty acid synthesis. *EBioMedicine*. 2019;40:251–262. https://doi.org/10.1016/j.ebiom.2018.12.037.
68. Fletcher JI, Haber M, Henderson MJ, Norris MD. ABC transporters in cancer: More than just drug efflux pumps. *Nat Rev Cancer*. 2010;10:147–156. https://doi.org/10.1038/nrc2789.
69. Holohan C, Van Schaeybroeck S, Longley DB, Johnston PG. Cancer drug resistance: an evolving paradigm. *Nat Rev Cancer*. 2013;13:714–726. https://doi.org/10.1038/nrc3599.
70. Yong L, Tang S, Yu H, et al. The role of hypoxia-inducible factor-1 alpha in multidrug-resistant breast cancer. *Front Oncol*. 2022;12. https://doi.org/10.3389/fonc.2022.964934.
71. Ozcan G. The hypoxia-inducible factor-1α in stemness and resistance to chemotherapy in gastric cancer: future directions for therapeutic targeting. *Front Cell Dev Biol*. 2023;11. https://doi.org/10.3389/fcell.2023.1082057.
72. Ezzeddini R, Taghikhani M, Salek Farrokhi A, et al. Downregulation of fatty acid oxidation by involvement of HIF-1α and PPARγ in human gastric adenocarcinoma and related clinical significance. *J PhysiolBiochem*. 2021;77:249–260. https://doi.org/10.1007/s13105-021-00791-3.
73. Ezzeddini R, Taghikhani M, Somi MH, Samadi N, Rasaee MJ. Clinical importance of FASN in relation to HIF-1α and SREBP-1c in gastric adenocarcinoma. *Life Sci*. 2019; 224:169–176. https://doi.org/10.1016/j.lfs.2019.03.056.
74. Brown JM, Giaccia AJ. The unique physiology of solid tumors: Opportunities (and problems) for cancer therapy. *Cancer Res*. 1998;58:1408–1416.
75. Li H, Sun X, Li J, et al. Hypoxia induces docetaxel resistance in triple-negative breast cancer via the HIF-1α/miR-494/Survivin signaling pathway. *Neoplasia*. 2022;32, 100821. https://doi.org/10.1016/j.neo.2022.100821.
76. Yang H, Geng Y-H, Wang P, Zhang H-Q, Fang W-G, Tian X-X. Extracellular ATP promotes breast cancer chemoresistance via HIF-1α signaling. *Cell Death Dis*. 2022; 13:199. https://doi.org/10.1038/s41419-022-04647-6.
77. Ding Z, Yang L, Xie X, et al. Expression and significance of hypoxia-inducible factor-1 alpha and MDR1/P-glycoprotein in human colon carcinoma tissue and cells. *J Cancer Res Clin Oncol*. 2010;136:1697–1707. https://doi.org/10.1007/s00432-010-0828-5.
78. Chen L, Feng P, Li S, et al. Effect of hypoxia-inducible factor-1α silencing on the sensitivity of human brain glioma cells to doxorubicin and etoposide. *Neurochem Res*. 2009;34:984–990. https://doi.org/10.1007/s11064-008-9864-9.
79. Liu L, Ning X, Sun L, et al. Hypoxia-inducible factor-1α contributes to hypoxia-induced chemoresistance in gastric cancer. *Cancer Sci*. 2008;99:121–128. https://doi.org/10.1111/j.1349-7006.2007.00643.x.
80. Lv Y, Zhao S, Han J, Zheng L, Yang Z, Zhao L. Hypoxia-inducible factor-1α induces multidrug resistance protein in colon cancer. *Onco Targets Ther*. 2015;8:1941–1948. https://doi.org/10.2147/OTT.S82835.
81. Krishnamurthy P, Ross DD, Nakanishi T, et al. The stem cell marker Bcrp/ABCG2 enhances hypoxic cell survival through interactions with heme. *J Biol Chem*. 2004; 279:24218–24225. https://doi.org/10.1074/jbc.M313599200.
82. He X, Wang J, Wei W, et al. Hypoxia regulates ABCG2 activity through the activivation of ERK1/2/HIF-1α and contributes to chemoresistance in pancreatic cancer cells. *Cancer Biol Ther*. 2016;17:188–198. https://doi.org/10.1080/15384047.2016.1139228.